

## Variability of sea surface salinity in stochastically forced systems

Michael A Spall

Clark 311A, Woods Hole Oceanographic Institution, Woods Hole, MA 02543, USA

Received January 30, 1992/Accepted August 6, 1992

**Abstract.** The influences of horizontal advection and horizontal diffusion on the variability of sea surface salinity in stochastically forced systems are investigated. Basic ideas are developed using a two dimensional box model and then extended to a more realistic three dimensional ocean general circulation model. It is shown that, in the absence of advection and diffusion, the ocean response is essentially that predicted by Taylor's random walk model. Advection becomes important when the advective time scale is less than the response time of the mixed layer to the stochastic forcing. Advection of parcels from regions of upwelling into regions of downwelling limits their exposure time to the stochastic forcing and thus the maximum attainable variance in the system (variance increases linearly with time). Regions of upwelling and downwelling may be introduced through the thermohaline overturning circulation or by the wind driven Ekman transport, depending on the specific model configuration. Horizontal diffusion is found to be important when the diffusive time scale is less than the mixed layer response time. The primary role of diffusion is to reduce the effective stochastic forcing through rapid mixing of uncorrelated surface forcing events. Because sea surface salinity does not have a negative feedback with the atmosphere, it is more strongly influenced by weak horizontal processes than sea surface temperature (SST). Accurate knowledge of the stochastic forcing amplitude, decorrelation time, and length scale and distribution are critical to model the variance of sea surface salinity. Aspects of the ocean model which strongly influence the variability of sea surface salinity include the surface velocity, horizontal diffusivity, and the mixed layer depth. Implications on modeling of the ocean and coupled ocean-atmosphere systems are discussed.

### Introduction

It is now generally believed that the oceanic thermohaline circulation is an important component of the global heat and fresh water budgets. One component of the global system, the North Atlantic circulation, transports significant amounts of heat towards the pole and fresh water towards the equator. It has been demonstrated in a wide variety of models, i.e., ocean box models (Marotzke 1990; Huang et al. 1992), ocean general circulation models (Marotzke 1990; Bryan 1986), coupled ocean-atmosphere box models (Birchfield 1989), and coupled ocean-atmosphere general circulation models (Manabe and Stouffer 1988), that the strength and even the sense of this basin scale overturning mode may undergo catastrophic change as a result of small variations in the sea surface salinity or flux of fresh water into the ocean at high latitudes. There has also been some speculation that this process may have been active in major climate changes in the past (i.e., the Younger-Dryas period, Broecker et al. 1985; Maier-Reimer and Mikolajewicz 1989). In addition, a global ocean general circulation model was found to have a dominant internal mode characterized by oscillations of the thermohaline circulation (Mikolajewicz and Maier-Reimer 1990) which was initiated by applying a sufficiently strong stochastic fresh water flux at the surface. Weaver et al. (1992) found that the strength of stochastic forcing strongly influenced the frequency and strength of events which release large amounts of heat into the atmosphere in a very short time. These previous studies demonstrate that the interaction of the general circulation with the surface salinity and fresh water fluxes are clearly important, timely, and very complex problems. We need to further our understanding of what determines the amplitude and distribution of variations in sea surface salinity and how this variability feeds back on the general ocean and coupled ocean-atmosphere systems. The present study addresses the first of these two issues.

The purpose of these calculations is not to simulate thermohaline catastrophies or determine the existence of multiple steady states. Because the onset of catastrophic

change is strongly dependent on the specific model physics, including model dimensions, surface forcing, mixed layer physics, subgridscale parameterizations, and model resolution, we seek a more general understanding of the mechanisms with control variance in a wide variety of stochastically forced models. The way in which this variance may interact with the ocean and coupled ocean-atmosphere systems to introduce abrupt change is, of course, a very important problem. However, it is emphasized here that in order to effectively study and predict change which results from stochastic fresh water flux forcing, one must first understand what controls the amplitude and distribution of the variability in surface salinity.

The starting point of the following discussion is the simple system where the surface salinity  $S$  is forced by a local fresh water flux  $p(t)$ , and  $S_t$  denotes the partial derivative of  $S$  with respect to  $t$ :

$$S_t = p(t) \tag{1}$$

This forcing is intended to represent the net effects of evaporation, precipitation, and ice melt at the surface. For statistically stationary forcing  $p(t)$ , the response is nonstationary with the variance increasing linearly in time for time scales long compared to the forcing time scale (Taylor 1921)

$$\langle S'^2 \rangle = 2Dt, \tag{2}$$

where  $S'$  is the deviation of salinity from the mean,  $\langle \cdot \rangle$  indicates the ensemble average, and

$$D = \frac{1}{2} \int_{-\infty}^{\infty} R(\tau) d\tau. \tag{3}$$

The parameter  $R$  is the covariance function defined as:

$$R(\tau) = \langle p(t+\tau)p(t) \rangle. \tag{4}$$

Early climate models have taken advantage of the separation in time scales between atmospheric forcing and oceanic response to demonstrate that the essentially red spectrum of low frequency oceanic variability is a natural response to a random white noise forcing by the atmosphere (Hasselmann 1976; Frankignoul and Hasselmann 1977). The present study builds on this previous work by seeking to determine the influences of horizontal advection, horizontal diffusion, and atmospheric forcing parameters on the amplitude of the sea surface salinity variability. This is an important next step in the path toward a general understanding of the variability of the oceanic thermohaline and coupled ocean-atmosphere general circulations, and in developing the ability to predict climate change. Knowledge of the critical parameters which control the amplitude of variability is necessary in order to effectively monitor, model, and study the ocean and coupled ocean-atmosphere climate systems.

The paper is outlined as follows. A two dimensional model of the thermohaline circulation is used in the second section to demonstrate the basic influences of horizontal advection and diffusion on the variability of sea surface salinity. In the third section these ideas are used

to interpret the salinity variance in three dimensional general circulation models and summary and discussion are presented in the final section.

### The meridional plane model

A simple two dimensional box model is used to investigate the basic consequences of horizontal advection and horizontal diffusion on the variance of sea surface salinity. Although such a model is clearly a very idealized representation of the actual ocean, it does provide a useful stepping stone between the single point mixed layer model of Hasselmann and the complex, three dimensional general circulation models used for predicting climate change. The insight gained from this simple model will be used in the next section to aid in the interpretation of more realistic general circulation model results.

### The numerical model

The model variables are horizontal velocity, vertical velocity, temperature, and salinity. The grid scheme is shown in Fig. 1. Each box is assumed to have uniform temperature  $T$  and salinity  $S$ . The horizontal velocity is calculated at the interfaces between density boxes and is proportional to the horizontal pressure gradient.

$$u = -cP_x \tag{5}$$

The proportionally constant  $c$  is a free parameter. A barotropic component of velocity is subtracted such that the depth integrated transport is zero. The vertical velocity into each grid box is calculated from the continuity equation

$$w_z = -u_x. \tag{6}$$

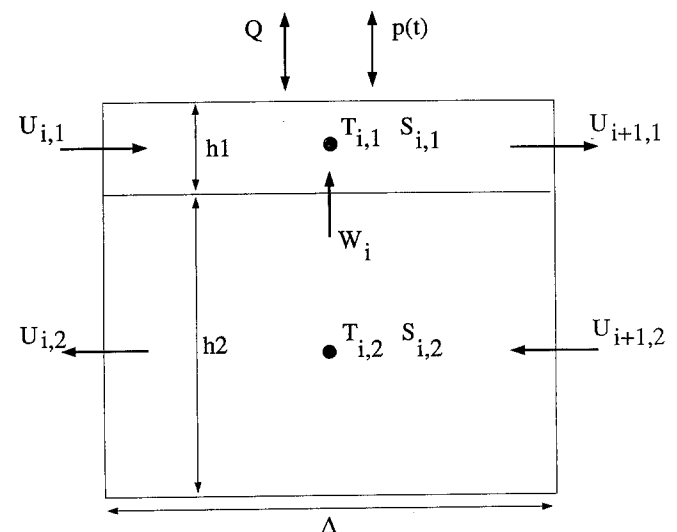


Fig. 1. Schematic of the box model for grid  $i$ . The two layers have thickness  $h_1$  and  $h_2$ . There are  $N = 10$  grid points in the horizontal each with uniform spacing  $\Delta$

The vertical velocity at the surface and bottom are zero. The density is calculated from a linear equation of state as

$$\rho = \beta S - \alpha T, \tag{7}$$

and the pressure is calculated from the hydrostatic relation

$$P_z = -g\rho \tag{8}$$

where  $g$  is the gravitational acceleration.

The temperature and salinity are calculated from advection/diffusion equations with surface forcing. Heat flux is parametrized by a relaxation condition proportional to the difference between the temperature of the surface box ( $T_s$ ) and a prescribed atmospheric temperature which is a linear function of latitude ( $T^*$ ). The time scale of the atmospheric feedback is  $\gamma$ . The salinity is forced at the surface through a prescribed flux which may be a function of time,  $p(t)$ . The horizontal Laplacian diffusion coefficient is denoted by  $K$ .

$$T_t + u T_x + w T_z = K T_{xx} + (T^* - T_s)/\gamma \tag{9}$$

$$S_t + u S_x + w S_z = K S_{xx} + p(t) \tag{10}$$

The model has solid walls at the northernmost and southernmost interfaces. The boundary conditions are no normal flow for velocity, no flux of temperature and salinity. This model is similar to that used by Huang et al. (1992) to study the stability and existence of various thermohaline modes which may exist with mixed boundary conditions.

The model is designed to approximately represent the meridional overturning circulation with the northward transport occurring in a relatively thin upper layer and a slower return flow of dense water in the thick deeper layer. It is intended to provide a means to understanding the basic consequences of horizontal processes on variability, not to give an actual prediction of the observed variability of sea surface salinity. It is inexpensive to run, thus allowing for many calculations and extensive exploration of parameter space. The model does not include rotational effects, wind forcing, and mixed layer physics. Although this makes it less realistic with respect to the real ocean, it does isolate the most basic consequences of the processes of interest.

**Parameter sensitivity**

For the experiments discussed here the density is assumed to be proportional to temperature only,  $\beta = 0$  in Eq. (7). Of course this limits much of the model physics and, in particular, prohibits the shutdown of deep water formation. This limitation of the model is justified here because we are not interested in the onset of the thermohaline catastrophe, or the existence of multiple equilibria states. The present simplified model allows us to explore a wider range of model parameters and to isolate the processes of interest more effectively than can be done with more complex models. The results found here are not qualitatively changed for small values of  $\beta$ , how-

ever the interpretation is clearer if we consider only the  $\beta = 0$  cases. The resulting velocity field is essentially constant so that the present analyses are relevant for other steady forcing mechanisms such as the wind driven Ekman transport.

The model is run under mixed boundary conditions with a restoring condition for temperature and a flux condition for salinity. The perturbation salinity flux is applied to the surface randomly in time in a series of uniform patches with length scale  $L$ . The value of the flux is constant over each patch and uncorrelated between adjacent patches. The amplitude of the perturbation is held fixed for  $\tau$  time units and then changed to a new random amplitude between  $\pm p$ . The Taylor diffusion coefficient for a single point exposed to this type of atmospheric forcing is calculated from Eqs. (3) and (4) as

$$D = \frac{1}{6} p^2 \tau. \tag{11}$$

Equation (2) indicates that the variance should increase linearly with  $D$ . This relation is tested in the box model by setting the horizontal advection and diffusion to zero ( $c = 0, K = 0$ ) and varying the amplitude  $p$  and decorrelation time  $\tau$  of the forcing. The results are shown in Fig. 2, where the variance plotted is the average of the variance in all of the upper layer boxes. The variance increase very nearly linearly with the Taylor diffusion coefficient  $D$ , as predicted by Eq. (2). Thus, in the absence of advection and diffusion, the upper ocean salinity responds to local stochastic forcing as the non-stationary integrated response to uncorrelated forcing events. Note that since there is no direct feedback between salinity and the atmosphere, in the absence of horizontal processes the salinity variance will grow unbounded. We will show that both horizontal advection

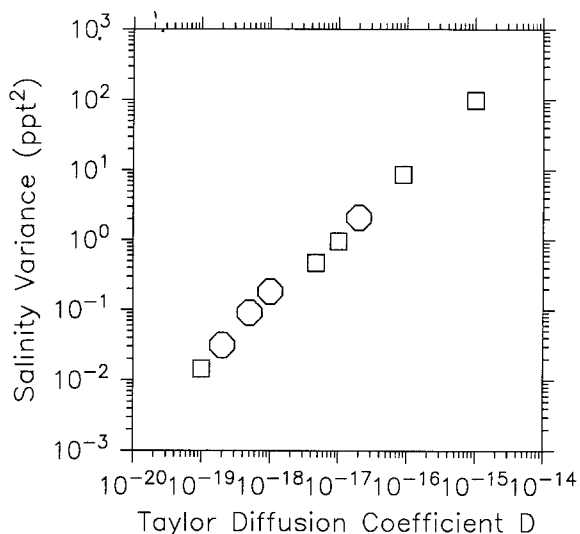


**Fig. 2.** Variance of sea surface salinity versus the Taylor diffusion coefficients  $D$ . The circles correspond to variations in the forcing amplitude between 3.7 mm month<sup>-1</sup> and 370 mm month<sup>-1</sup> with  $\tau$  fixed at 36.5 days and the squares correspond to variations in the decorrelation time between 36.5 days and 20 years with the forcing amplitude fixed at 3.7 mm month<sup>-1</sup>

and horizontal diffusion limit the maximum attainable variance through two very different mechanisms.

The influences of advection and diffusion, and their relationship to the scale of the atmospheric forcing, can be more fully understood if we consider the nondimensional form of the layer 1 salinity equation.

$$S_t = -uS_x - wS_z - \frac{K}{VL} \nabla^2 S + \frac{LE}{VH} r(t) \quad (12)$$

The length scale of the atmospheric forcing is  $L$ ,  $V$  is the characteristic horizontal velocity,  $H$  is the depth of the mixed layer, and  $E$  is the amplitude of the stochastic forcing, and  $r(t)$  is a random number between  $\pm 1$ . The coefficient in front of the stochastic forcing term measures the relative influence of random forcing compared to advection. It may be thought of as the advective time scale over the time scale of the mixed layer response to the atmospheric forcing. The ratio of the stochastic forcing term to the diffusive term is a measure of the relative importance of diffusion and may be interpreted as the diffusive time scale over the stochastic forcing time scale. Thus, the relative influences of advection and diffusion are measured by the time scale ratios  $\tau_a$  and  $\tau_d$ , where

$$\tau_a = \frac{VH}{EL}, \quad \tau_d = \frac{KH}{EL^2}. \quad (13)$$

Increasing the mixed layer depth, or decreasing the forcing amplitude, decreases the effective forcing in both advective and diffusive systems. Increasing the velocity or decreasing the length scale of the atmospheric forcing increases the importance of advection, while increasing the diffusion coefficient or decreasing the length scale of the atmospheric forcing increases the importance of diffusion. Analogous time scale ratios may be calculated for the variability of SST which are appropriate for time scales less than the feedback time scale with the atmosphere.

Before moving on to the general advective/diffusive problem, we first start with two simpler systems by initially neglecting advection and then neglecting diffusion. A series of calculations have been done in which  $c=0$  and the diffusion coefficient  $K$  and the atmospheric forcing scale  $L$  are varied, the results are shown in Fig. 3a. Small values of  $\tau_d$  indicate that the diffusive time scale is much larger than the forcing time scale and the variance is the same as for the single point model ( $D=10^{-19}$  in Fig. 2), independent of diffusion. As  $\tau_d$  becomes greater than 1 the diffusion becomes important and the variance is decreased. This may be thought of as the oceanic response to an atmospheric forcing which is effectively decreased through rapid horizontal mixing across the forcing decorrelation scale. For sufficiently large  $K$  the effects of the finite basin size become important and variance approaches a steady amplitude which is independent of  $K$  but dependent on  $L$ . In the large  $K$  limit, the effective forcing is reduced by  $L/N\Delta$  (because there are that many uncorrelated forcing events in the basin) and the ocean response is reduced by  $(L/N\Delta)^2$ , compared to the inviscid limit. It is important to note

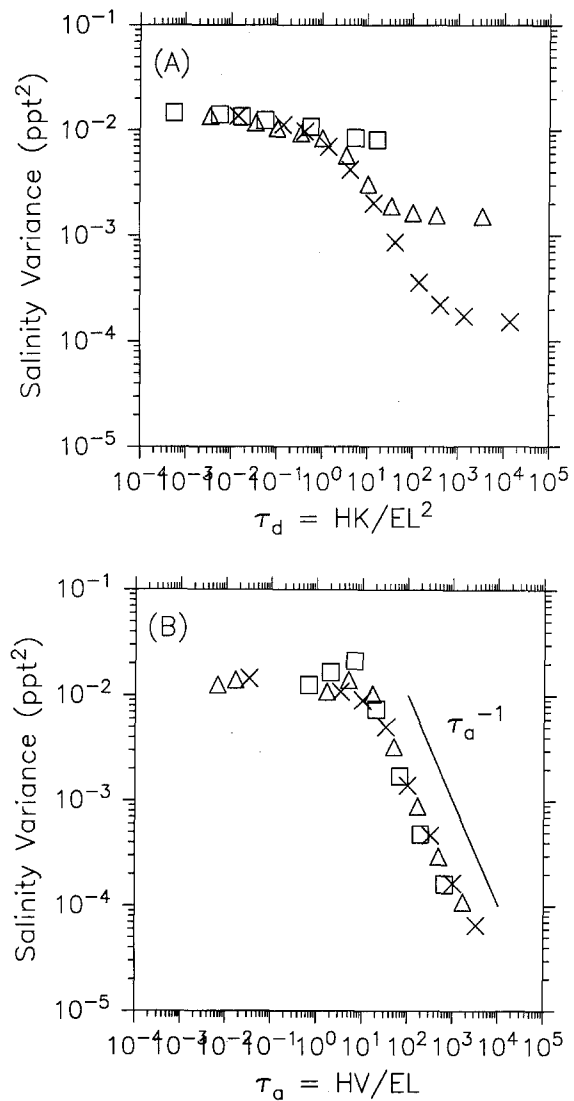


**Fig. 3.** A, B. Variance of sea surface salinity versus **A** diffusive time scale  $\tau_d$ ; **B** advective time scale  $\tau_a$ . Symbols  $\times$  indicates  $L=1$  grid space;  $\Delta$  indicates  $L=2$ ; and  $\square$  indicates  $L=5$

that this effect is independent of the specific form of the horizontal mixing.

We now investigate the influence of horizontal advection in the absence of diffusion by setting  $K=0$  and varying  $c$  and  $L$ , the results are shown in Fig. 3b. For very small values of  $\tau_a$  the variance is independent of the forcing scale and the same as the single point model. The variance remains approximately constant until  $\tau_a$  is greater than one. At  $\tau_a=1$  the time it takes to advect a parcel horizontally across the scale of the atmospheric forcing is the same as the time scale of the surface salinity response to stochastic forcing of amplitude  $E$ . Beyond this value, the variance decreases linearly with increasing  $\tau_a$ . As the horizontal advection speed increases, the parcels are exposed to the atmospheric forcing for shorter amounts of time, i.e., the amount of time it takes for a parcel to be advected from equator to pole. The linear decay is simply the result of the linear relationship between the variance and time in the simple stochastically forced system (Eq. 2).

## A general circulation model

The results from the previous section related the relative influences of horizontal advection and diffusion to the inherent time scales of a very simple two dimensional system. We are interested in how these basic ideas carry over into a more realistic application which includes a three dimensional ocean, wind forcing, convective overturning, large-scale mean fresh water flux, variable depth mixed layer, and a general equation of state. While the main focus of this study is to expose the basic consequences of horizontal processes, it is important to demonstrate how the concepts developed with the very idealized model manifest themselves in the more general case.

We use the version of the GFDL primitive equation general circulation model distributed by Pacanowski et al. (1991 unpublished manuscript), which is based on the model documented by Cox (1984) and the equations described by Bryan (1969). The ocean basin is a  $67.5^\circ$  wide section which extends from the equator to  $72^\circ\text{N}$  and has a 4500 m flat bottom. The horizontal resolution is  $3.75^\circ$  in longitude and  $4^\circ$  in latitude and there are 15 levels in the vertical with grid spacing increasing from 50 m near the surface to approximately 570 m in the deep ocean. Statically unstable density profiles are treated by increasing the vertical diffusion coefficient to  $1000 \text{ cm}^2 \text{ s}^{-1}$ , elsewhere it is constant at  $0.5 \text{ cm}^2 \text{ s}^{-1}$ . The horizontal coefficients of viscosity and diffusivity are  $2.5 \times 10^9 \text{ cm}^2 \text{ s}^{-1}$  and  $1 \times 10^7 \text{ cm}^2 \text{ s}^{-1}$ , respectively, and the vertical coefficient of viscosity is  $1.0 \text{ cm}^2 \text{ s}^{-1}$ . The model is forced with a zonal wind stress which approximates the zonally averaged wind stress over the North Atlantic, Fig. 4. This configuration is very similar to several previous general circulation models which have been used for climate studies (e.g., Bryan 1986; Marotzke 1990; Weaver et al. 1992) and the resolution is close to what is commonly used in coupled ocean-atmosphere general circulation models.

The surface heat flux is parameterized by a relaxation of the temperature in the uppermost grid box to a zonally uniform "atmospheric" temperature ( $T^*$ ) which de-

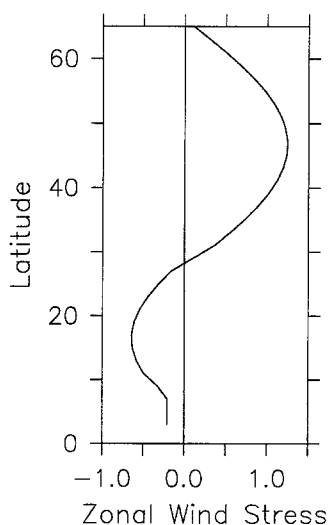


Fig. 4. Meridional distribution of zonal surface wind stress (dynes)

creases from  $27^\circ\text{C}$  at the equator to  $0^\circ\text{C}$  at  $72^\circ\text{N}$  following the cosine law

$$T^*(y) = 27(1 + \cos(y\pi/L))/2. \quad (14)$$

The surface heat flux in the ocean is reasonably parameterized as being proportional to the difference between the ocean sea surface temperature and the atmospheric temperature. The atmospheric forcing for salinity is nearly independent of the sea surface salinity, so that a similar relaxation approach is not appropriate. However, the mean evaporation minus precipitation at the ocean surface (E-P) is not well known and the southward transport of fresh water in the slope region off the continental United States is not well represented in such large-scale models. We follow the traditional modeling approach by initially running the model with a relaxation condition on the sea surface salinity until the model arrives at a steady state (10000 years). The form of the relaxation salinity is

$$S^*(y) = 33.5 + 2.5(1 + \cos(y\pi/L))/2, \quad (15)$$

which gives a maximum salinity at low latitudes and a minimum at high latitudes. The relative changes in surface temperature and salinity from equator to pole would indicate that the sea surface salinity is important to, but does not dominate, the state of the thermohaline circulation (Weaver et al. 1991). The mean E-P at the surface ( $\bar{p}$ ) is diagnosed from the steady model fields and specified as a mean flux condition for the perturbation experiments. The model is then run for an additional 2500 years under mixed boundary conditions, relaxation for temperature and flux for salinity. The model circulation remains essentially constant for the 2500 years when forced by the relaxation on temperature and the mean flux condition for salinity with no perturbation added.

Each of the stochastic forcing experiments discussed in this section undergoes a transition from the initial spinup state to another, slightly different, steady state under the flux boundary conditions for salinity. The strength of the meridional overturning cell increases from  $8.5 \times 10^6 \text{ m}^3 \text{ s}^{-1}$  to  $12 \times 10^6 \text{ m}^3 \text{ s}^{-1}$  over the first several hundred years. The upper ocean generally becomes fresher and the deep ocean becomes saltier. This transition also occurs when a fresh water anomaly is added to the surface layer at high latitudes upon switching to flux boundary conditions, even when the forcing remains steady. A similar shift between steady states was found by Marotzke (1990) and Weaver et al. (1991) under steady forcing. It is concluded that this transition is characteristic of the model response to mixed boundary conditions, it is not dependent on the nature of the stochastic forcing, and it will not be discussed further here.

### Parameter sensitivity experiments

A series of stochastically forced experiments have been carried out starting at year 10000 under mixed boundary conditions. The fresh water flux at the surface is specified

as the mean ( $\bar{p}$ ) plus a random perturbation ( $p$ ). Following the two dimensional model, the perturbation flux is assumed to be uniform over a horizontal length scale  $L$  (now in the zonal and meridional directions) and is uncorrelated at distances greater than  $L$ . The anomalous E-P events persist for a period of  $\tau$  time units and then attain a new, uncorrelated amplitude for the next  $\tau$  time units. We are interested in the variability of sea surface salinity as a function of the perturbation length scale  $L$ , its amplitude  $p$  and time scale  $\tau$ , and the model horizontal diffusion  $K$ .

The central experiment is forced with a random E-P of amplitude  $\pm 30$  mm month<sup>-1</sup> and a decorrelation time scale of  $\tau = 4$  days. This amplitude is approximately 35% of the RMS E-P over the North Atlantic and represents a relatively weak, but realistic, input by random storms, ice melt, and evaporation. Although such homogeneous forcing is idealized with respect to the actual forcing, we use it here because it lends itself to analysis in terms of simple models and is in keeping with the present process oriented approach. The time scale ratios discussed in the previous section are now calculated for the three dimensional model. The advective time scale ratio  $\tau_a = VH/EL = 125$  indicates that the advective time scale is much shorter than the response time to the atmospheric forcing, so we expect that horizontal advection is limiting the amplitude of the variance. The diffusive time scale  $\tau_d = KH/EL^2 = 31$  for forcing on a one grid point scale and  $\tau_d = 0.1$  for forcing on the basin scale. Thus, for small-to intermediate-scale forcing, the diffusive time scale is also much less than the forcing scale so we expect that horizontal mixing by the subgrid-scale diffusion will reduce the effective amplitude of the stochastic forcing for these cases.

We first want to see if Taylor's model holds for the more general ocean model used here or if other proc-

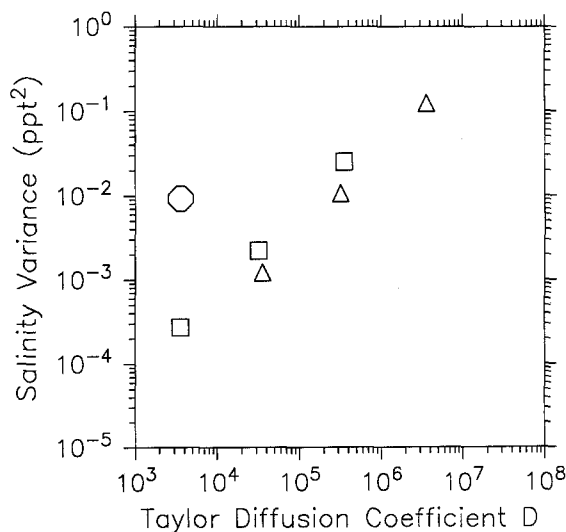


**Fig. 5.** Variance of sea surface salinity in the general circulation model versus the Taylor diffusion coefficient  $D$ . The squares and triangles correspond to experiments with  $\tau = 4$  days and  $\tau = 40$  days, respectively, and forcing amplitudes of 30 mm month<sup>-1</sup>, 90 mm month<sup>-1</sup> and 300 mm month<sup>-1</sup>. The circle marks the variance in the single point Taylor model

esses, such as internal variability, are dominant. The variability of the sea surface salinity as a function of the Taylor diffusion coefficient  $D = \frac{1}{8} p^2 \tau$  is shown in Fig. 5. The variance has been averaged between 4°N and 60°N at -35°W, this longitude was chosen as representative of the ocean interior, away from boundary influences. There is a nearly linear relationship between variance and the diffusion coefficient, similar to that found for the two dimensional model and in agreement with the simple single point theory. We note, however, that the variance predicted by the single point model (indicated by the circle) is approximately 35 times larger than that found in the general circulation model with the same stochastic forcing. This is very close to the factor of 30 predicted by the two dimensional box model for  $\tau_a = 125$ ,  $\tau_d = 31$  in Fig. 3a,b and indicates that horizontal processes are strongly limiting the variability of sea surface salinity in the three dimensional model.

A direct comparison of these results with observations is not done here both because of the process oriented nature of the analysis and the lack of extensive time series of sea surface salinity. The amplitude of the salinity anomaly predicted by the GCM with reasonable atmospheric forcing parameters is approximately 0.05 ppt, in general agreement with the observations in the subpolar gyre (Taylor and Stephens 1980). Several studies based on observations (Frankignoul and Reynolds 1982; Herterich and Hasselmann 1987; Bryan and Stouffer 1991) indicate that, in addition to stochastic forcing by the atmosphere, horizontal advection may be important in the balance of SST anomalies. This indicates that the advective time scale is less than the SST feedback time scale which, in turn, implies that advection is also important to the variability of sea surface salinity.

The variance found here is a direct response to the stochastic forcing, it does not represent the natural internal variability of the model under steady forcing. To demonstrate this, stochastic forcing was set to zero well after the initial adjustments of the thermohaline circulation (500 years). The resulting salinity variance was more than two orders of magnitude less than that for the stochastically forced case. We also note that the thermohaline mode does not undergo any catastrophic collapse as a result of the stochastic forcing for the parameter ranges reported here. Other model configurations, however, can result in a shutdown of the overturning mode for similar forcing parameters.

#### *Distribution of salinity variance*

It was shown in the previous section that surface variability may be limited by horizontal advection if the horizontal motion carries surface parcels into regions of downwelling and removes them from the atmospheric forcing. In the two dimensional model this was achieved with a very idealized thermohaline overturning cell. It is now demonstrated that the wind and buoyancy driven surface velocity serves the same purpose in the three dimensional general circulation by carrying surface parcels

from regions up upwelling near the equator and pole into a region of downwelling in the subtropical convergence zone.

The response of a Lagrangian parcel exposed to stochastic forcing, in the absence of horizontal mixing processes, is the same as the Eulerian response described by Eq. (2). For horizontally homogeneous forcing in the inviscid limit one would then expect to find a minimum in surface variance in regions where the parcels are first exposed to the atmosphere and a maximum in the region where parcels have been exposed to the atmospheric forcing for the longest amount of time. For the zonal wind stress representative of that over the North Atlantic there are regions of upwelling at high and low latitudes and a region of maximum downwelling in the subtropical convergence zone, near 25°N.

In order to test this hypothesis, we would like to compare the development of the salinity variance following a parcel trajectory at the surface with that which is calculated from the single point model exposed to the same atmospheric forcing. Since we can not integrate the model without horizontal diffusion, we approach an effective inviscid limit by decreasing  $\tau_d$  (increasing the length scale of the atmospheric forcing  $L$ ). This will increase the time scale of the relevant horizontal diffusion process and thus minimize its influence on the variance following the parcel trajectory. The model was run with forcing parameters  $p = 30 \text{ mm month}^{-1}$ ,  $\tau = 4 \text{ days}$ , and  $L = 72^\circ$ , giving  $\tau_d = 0.1$ . The resulting variance of sea surface salinity is shown in Fig. 6a, calculated over the final 1500 years of integration. The bold lines indicate the horizontal trajectories of two parcels introduced at the surface, one in the subpolar gyre and one in the subtropical gyre, and advected with the mean horizontal velocity field.

The variance is quite large near 50°N, 55°W where the fresh subpolar gyre water meets the saline subtropical gyre water as it separates from the western boundary. Small variations in the position of this merger give rise to vary large salinity variance. The variance is also large along the eastern boundary near 40°N. This is where the deep vertical convective region which characterizes the subpolar gyre and the nonconvective region which characterizes the subtropical gyre meet the eastern boundary. The surface salinity adjacent to the solid boundary switches between a fresh value when convection is not active, and a saline value when the column vertically mixes. It is possible that both of these large variances are related to the weak horizontal advection processes in each region (see Fig. 6b), however, they are not representative of the large scale balances and will not be considered in detail here.

The interior of the basin shows minima in the subtropical and subpolar gyres away from the boundary. The variance increases toward the middle of the basin near 23°N, and toward the eastern boundary in the subtropical gyre. Figure 6b shows the mean horizontal velocity at the uppermost level in the model. The western boundary current and wind forced Ekman transports dominant the velocity field. The wind driven transport is to the south in the subpolar gyre and to the north in the

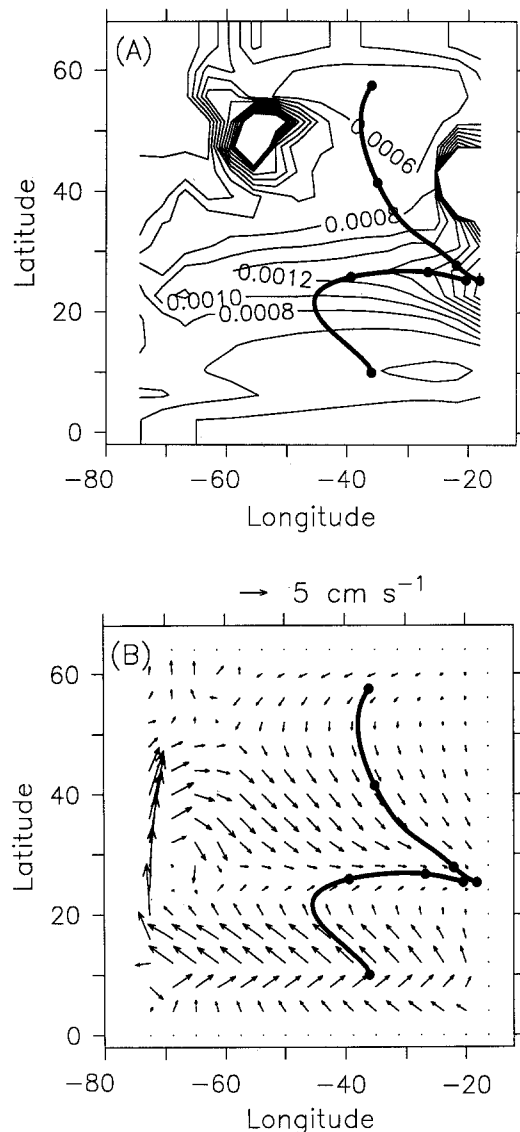


**Fig. 6.** **A** Variance of sea surface salinity in the general circulation model ( $\text{ppt}^2$ ) over the final 1500 years of integration; **B** mean surface velocity field (the contour level has been limited to .0025 for clarity). **Bold line** indicates surface parcel trajectories with **circles** placed at four year increments

subtropical gyre. The subtropical convergence zone is clear near 23°N. There is also an eastward component which results from the geostrophic balance with the meridional temperature gradient, forcing a convergence in the eastern portion of the subtropical gyre. A general trend of increasing variance with increasing exposure time is indicated by the parcel trajectories.

The Lagrangian interpretation is quantified by comparing the model variance interpolated along each of the parcel trajectories with that which is calculated from the simple single point model given by Eqs. (2) and (3) over the same time period. The ocean general circulation model is forced by a net fresh water flux at the surface. The influence of this fresh water flux on the salinity over the depth of the mixed layer is calculated as

$$p = \frac{ES_0}{H} \quad (16)$$

Where  $S_0$  is the surface salinity and  $H$  is the local mixed layer depth. Equation (2) is integrated along the parcel trajectory using this effective forcing  $p$ . Although the maximum attainable amplitude of the fresh water flux  $E$  is uniform in time, the effective forcing  $p$ , and thus the resulting Taylor diffusion coefficient, may be variable because the mixed layer depth  $H$  can vary with position (and hence time following the parcel). At high latitudes the mixed layer depth is deep and the effective forcing is reduced while at mid and low latitudes the mixed layer depth is shallow and the effective forcing is increased.

The variance interpolated from the model grid following the parcel trajectory is indicated in Fig. 7a by the solid lines and the single point model integration is indicated by the dashed lines. There are several interesting results which are summarized in this figure. First, and

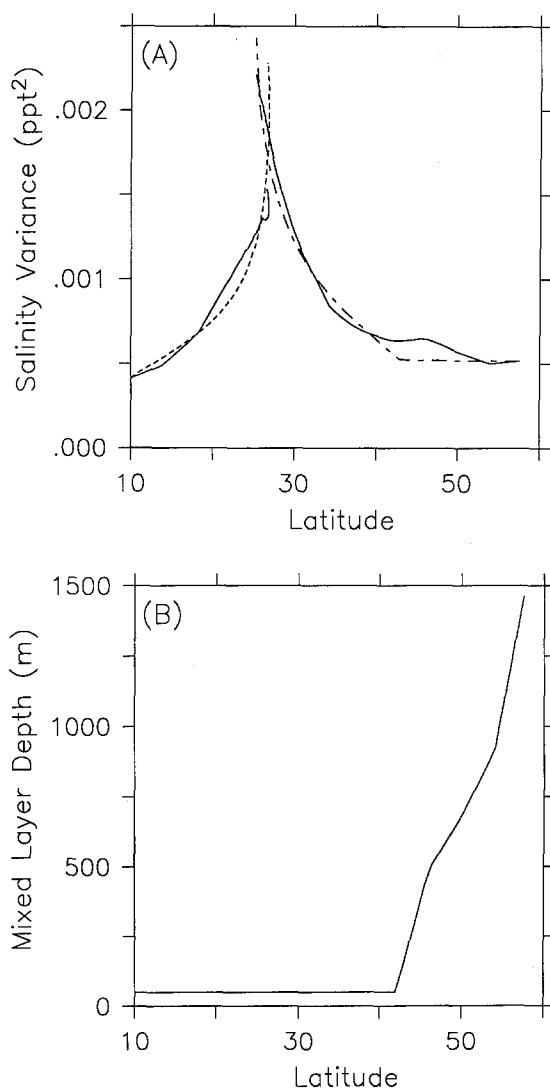


**Fig. 7.** **A** Variance following two Lagrangian paths, *solid lines* indicate variance in the general circulation model, *dashed lines* indicate variance calculated from Taylor's random walk model following each parcel; **B** mixed layer depth versus latitude following the Lagrangian parcels

most importantly, the Lagrangian application of the random walk model gives a good approximation to both the structure and amplitude of the variance found in the three dimensional model. The minima at high and low latitudes and the sharp front located at the latitude of the subtropical convergence zone are all reproduced. Away from the boundary regions, the surface variance increases nearly linearly with the time that the parcels are exposed to surface forcing. The two dimensional pattern seen in Fig. 6a is simply a reflection of the two dimensional nature of the surface velocity field. The variance in the subpolar gyre is nearly constant, as reflected by the slow growth following the subpolar gyre parcel between 60°N and 40°N. Although the parcel spends approximately 33% of its time at the surface north of 40°N, less than 10% of the total increase in variance is experienced in this region. This is explained if we consider the mixed layer depth following the parcel trajectories in Fig. 7b. The nearly uniform variability at high latitudes is a result of the reduction in effective forcing where the mixed layer is deep, i.e., the fresh water input is mixed over a larger amount of the water column so the net influence on salinity is reduced. The Lagrangian single point model predicts this nearly uniform variance at high latitudes fairly well. Once the parcel is south of 40°N, the mixed layer rapidly shallows to 50 m and the variance begins to increase. The strong front indicated at the latitude of the subtropical convergence zone results from the parcels in this region being exposed to the stochastic forcing for the longest amount of time. The general increase toward the east along the subtropical convergence zone is a result of the eastward component of the surface velocity (balanced by the large-scale meridional density gradient) prolonging the exposure time at the surface.

### Summary and discussion

The results presented in the two previous sections give a consistent interpretation of the influences of advection and diffusion on the variability of sea surface salinity. Two models were used, a two dimensional box model and a three dimensional ocean circulation model. The model configurations were simplified to the extent necessary to illustrate the processes of interest, while still retaining relevance both to the real ocean and to a variety of models used to study climate systems. The primary influence of horizontal advection is to remove parcels from the atmospheric forcing by carrying them from regions of upwelling into regions of downwelling. These regions may result as a consequence of the thermohaline circulation or the wind driven Ekman transport, depending on the model configuration. Horizontal diffusion limits the variability by reducing the effective forcing through rapid mixing of uncorrelated surface forcing events. The relative influences of advection and diffusion are measured by nondimensional numbers  $\tau_a$  and  $\tau_d$ , which are the ratios of the response time of the stochastically forced upper mixed layer to the advective and diffusive time scales, respectively. In the limit of



small  $\tau_a$  and  $\tau_d$  the variance of sea surface salinity is accurately represented by the random walk model of Taylor (Taylor 1921). Even with large  $\tau_a$  and  $\tau_d$ , the random walk model is still valid with the appropriately reduced effective forcing period or amplitude.

The implications of these results are that the variance of sea surface salinity is very sensitive to the atmospheric forcing parameters and ocean circulation physics. Unfortunately, the flux of fresh water is one of the least well-known quantities in the ocean. The validity of the random walk model indicates that the variance is proportional to the square of the amplitude of the fresh water flux so that, as expected, this is a very important quantity in determining the upper ocean variability. However, the length scale of the forcing events may also be quite important, particularly when diffusion is strong enough to effectively mix surface forcing events ( $\tau_d > 1$ ). If strong fresh water flux events take place along small scale atmospheric fronts, because  $\tau_d \sim L^{-2}$ , then even relatively weak horizontal mixing may strongly limit the resulting variance. The variance also increases linearly with the decorrelation time of the forcing events. If rain storm events take place on time scales of  $O$  (days), then models which would otherwise permit time steps longer than this may be constrained by this time scale. However, the present results suggest that one may obtain the same effective forcing with an increase in the decorrelation time, if there is a corresponding decrease in the amplitude of the forcing, such that the Taylor diffusion coefficient remains constant. The ocean model physics are also important in determining the amplitude and pattern of salinity variability, especially critical components include the surface velocity, model diffusivity, and mixed layer depth.

In the advective inviscid limit, the variance of sea surface salinity is essentially the integrated response to the local atmospheric forcing following the parcel trajectory. The effective forcing may be a function of position either through a variable depth mixed layer, as in the present study, or through non-homogeneous stochastic forcing. This implies that the distribution of salinity variance is determined both by the local forcing and by the time history of the forcing which the Lagrangian parcels have experienced upstream. Near surface currents are strongly influenced by the Ekman drift, so that both large-scale wind forcing and the geostrophic flow are important to the pattern of salinity variability. In the present general circulation model forced with winds representative of the North Atlantic, the salinity variance is a minimum at high and low latitudes, where parcels are upwelled to the surface, and a maximum in the subtropical convergence zone, where parcels have been exposed to the atmosphere for the longest amount of time before being removed from the surface layer. The variance at high latitudes is further minimized by a deep mixed layer depth, which reduces the effective amplitude of the stochastic forcing. The time required for a parcel to be advected from either high latitudes or low latitudes into the STCZ is  $O$  (10 years), so that the surface variance in long model integrations can not grow beyond that which can accumulate over this time scale.

There are interesting similarities and differences between the role of horizontal processes in the variability of sea surface salinity (SSS) and SST. For time scales less than the feedback time scale with the atmosphere, randomly forced SST will be influenced in the same way as randomly forced SSS and time scale ratios analogous to those presented here may be calculated. However, unlike SST, SSS variance will grow unbounded in the absence of non-local processes because there is no negative feedback with the atmosphere. Thus, even weak horizontal processes, which may not be important for SST variability, are very important for SSS because they provide a mechanism which limits the variability on long time scales.

*Acknowledgements.* This work was supported by NOAA Grant No. NA90AA-D-AC498 under the Atlantic Climate Change Program. The ocean general circulation model calculations were carried out at the National Center for Atmospheric Research, which is sponsored by the National Science Foundation, under the University Research and Development Grant Program sponsored by Cray Research, Inc. The author would like to thank Ron Pacanowski, Keith Dixon, and Anthony Rosati at the Geophysical Fluid Dynamics Laboratory for providing the Modular Ocean Model version of the GFDL ocean general circulation model. This is Woods Hole Oceanographic Institution contribution number 7952.

## References

- Birchfield GE (1989) A coupled ocean-atmosphere climate model: temperature versus salinity effects on the thermohaline circulation. *Clim Dyn* 4:57-71
- Broecker WS, Peteet DM, Rind D (1985) Does the ocean-atmosphere have more than one stable mode of operation? *Nature* 315:21-26
- Bryan FO (1986) High latitude salinity effects and intrahemispheric thermohaline circulation. *Nature* 323:301-304
- Bryan K (1969) A numerical method for the study of the circulation of the world ocean. *J Comput Phys* 4:347-376
- Bryan K, Stouffer R (1991) A note on Bjerknes' hypothesis for North Atlantic variability. *J Mar Syst* 1:229-241
- Cox MD (1984) A primitive equation, 3-dimensional model of the ocean. GFDL Ocean Group Tech Rep No. 1
- Frankignoul C, Hasselmann K (1977) Stochastic climate models, Part II. Application to sea-surface temperature anomalies and thermocline variability. *Tellus* 29:289-305
- Frankignoul C, Reynolds RW (1982) Testing a dynamical model for mid-latitude sea surface temperature anomalies. *J Phys Oceanogr* 13:1131-1145
- Hasselmann K (1976) Stochastic climate models. Part I. Theory. *Tellus* 28:473-485
- Herterich K, Hasselmann K (1987) Extraction of mixed layer advection velocities, diffusion coefficients, feedback factors, and atmospheric forcing parameters from the statistical analysis of North Pacific SST anomaly fields. *J Phys Oceanogr* 17:2145-2156
- Huang RX, Luyten JR, Stommel HM (1992) Multiple equilibrium states in combined thermal and saline circulation. *J Phys Oceanogr* 22:231-246
- Maier-Reimer E, Mikolajewicz U (1989) Experiments with OGCM on the cause of the Younger Dryas. Ayala-Castanares A, Wooster W, Yanez-Arancibia A (eds) *Oceanography 1988*. UNAM Press, Mexico DF
- Manabe S, Stouffer R (1988) Two stable equilibria of a coupled ocean-atmosphere model. *J Clim* 1:841-866

- Marotzke J (1990) Instabilities and multiple steady states of the thermohaline circulation. PhD Thesis, Ber Institut für Meereskunde, Kiel, June 1990
- Mikolajewicz U, Maier-Reimer E (1990) Internal secular variability in an ocean general circulation model. *Clim Dyn* 4:145-156
- Taylor AH, Stephens JA (1980) Seasonal and year-to-year variations in surface salinity at the nine North Atlantic Ocean weather stations. *Oceanol Atca* 3:421-430
- Taylor GI (1921) Diffusion by continuous movements. *Proc Lond Math Soc* 20:196
- Weaver AJ, Marotzke J, Cummins PF, Sarachik ES (1992) Stability and variability of the thermohaline circulation. *J Phys Oceanogr* (in press)
- Weaver AJ, Sarachik ES, Marotzke J (1991) Freshwater flux forcing of decadal/interdecadal oceanic variability. *Nature* 353:836-838